

# Astronomical Notes

## Astronomische Nachrichten

Founded by H. C. Schumacher in 1821

### Editors

K. G. Strassmeier (Potsdam/Editor-in-Chief),  
G. Hasinger (Garching), R.-P. Kudritzki (Honolulu),  
T. Montmerle (Grenoble), H. W. Yorke (Pasadena)

 **WILEY-VCH**

**REPRINT**

# Galactic Sun's motion in the cold dark matter, MODified Newtonian Dynamics and modified gravity scenarios

L. Iorio\*

INFN-Sezione di Pisa, Viale Unità di Italia 68, I-70125 Bari, Italy

Received 2009 Mar 9, accepted 2009 Jul 16

Published online 2009 Sep 20

**Key words** celestial mechanics, stellar dynamics – cosmology: dark matter – Galaxy: solar neighborhood – gravitation

We numerically integrate the equations of motion of the Sun in Galactocentric Cartesian rectangular coordinates for  $-4.5 \text{ Gyr} \leq t \leq 0$  in Newtonian mechanics with two different models for the Cold Dark Matter (CDM) halo, in MODified Newtonian Dynamics (MOND) and in MODified Gravity (MOG) without resorting to CDM. The initial conditions used come from the latest kinematical determination of the 3D Sun's motion in the Milky Way (MW) by assuming for the rotation speed of the Local Standard of Rest (LSR) the recent value  $\Theta_0 = 268 \text{ km s}^{-1}$  and the IAU recommended value  $\Theta_0 = 220 \text{ km s}^{-1}$ ; the Sun is assumed located at 8.5 kpc from the Galactic Center (GC). For  $\Theta_0 = 268 \text{ km s}^{-1}$  the birth of the Sun, 4.5 Gyr ago, would have occurred at large Galactocentric distances (12–27 kpc depending on the model used), while for  $\Theta_0 = 220 \text{ km s}^{-1}$  it would have occurred at about 8.8–9.3 kpc for almost all the models used. The integrated trajectories are far from being circular, especially for  $\Theta_0 = 268 \text{ km s}^{-1}$ , and differ each other with the CDM models yielding the widest spatial extensions for the Sun's orbital path.

© 2009 WILEY-VCH Verlag GmbH & Co. KGaA, Weinheim

## 1 Introduction

In several astrophysical systems like, e.g., spiral galaxies and clusters of galaxies a discrepancy between the observed kinematics of their exterior parts and the predicted one on the basis of the Newtonian dynamics and the matter detected from the emitted electromagnetic radiation (visible stars and gas clouds) was present since the pioneering studies by Zwicky (1933) (he postulated the existence of undetected, baryonic matter; today, it is believed that the hidden mass is constituted by non-baryonic, weakly interacting particles) on the Coma cluster, and by Bosma (1981) and Rubin et al. (1982) on spiral galaxies. More precisely, such an effect shows up in the galactic velocity rotation curves (Persic & Salucci 1996a, 1996b) whose typical pattern after a few kpc from the center differs from the Keplerian  $1/\sqrt{r}$  fall-off expected from the usual dynamics applied to the electromagnetically-observed matter.

As a possible solution of this puzzle, the existence of non-baryonic, weakly-interacting Cold Dark (in the sense that its existence is indirectly inferred only from its gravitational action, not from emitted electromagnetic radiation) Matter (CDM) was proposed to reconcile the predictions with the observations (Rubin 1983) in the framework of the standard gravitational physics.

Oppositely, it was postulated that the Newtonian laws of gravitation have to be modified on certain acceleration scales to correctly account for the observed anomalous kinematics of such astrophysical systems without resorting to

still undetected exotic forms of matter. One of the most phenomenologically successful modification of the inverse-square Newtonian law, mainly with respect to spiral galaxies, is the MODified Newtonian Dynamics (MOND) (Milgrom 1983a, 1983b, 1983c) which, as we will see below, yields a  $\approx 1/r$  gravitational force for very small accelerations.

Another alternative theoretical framework recently put forth to also explain, among other astrophysical and cosmological observations, the observed kinematics of the outskirts of galaxies without resorting to CDM is MODified Gravity (MOG) (Moffat & Toth 2008) which yields a long-range Yukawa-like modification of the Newtonian inverse-square law.

In this paper we want to investigate the motion of the Sun in the Milky Way (MW) over timescales of the order of its lifetime, i.e. 4.5 Gyr, in CDM, MOND and MOG scenarios in view of the recent accurate measurements of the solar kinematical parameters (Reid et al. 2009). This may help in discriminating, at least in principle, the different theoretical scenarios examined; moreover, it will be interesting to see if the Galactic orbital motions of the Sun backward in time predicted by CDM, MOND and MOG are compatible with known and accepted knowledge concerning its formation and the evolution of the life in our planet. This may also yield an independent consistency test of the new kinematical determinations of MW (Reid et al. 2009). Finally, we note that the approach presented here may be used, in principle, also for other dynamical features.

\* Corresponding author: lorenzo.iorio@libero.it

**Table 1** Parameters of the disk and bulge models by Xue et al. (2008).

$M_{\text{disk}}$ ( $M_{\odot}$ )	$M_{\text{bulge}}$ ( $M_{\odot}$ )	$b$ (kpc)	$c_0$ (kpc)
$5 \times 10^{10}$	$1.5 \times 10^{10}$	4	0.6

**Table 2** Parameters of the CDM NFW halo model by Xue et al. (2008). The values quoted for  $r_{\text{vir}}$  and  $c$  come from an average of those by Xue et al. (2008).

$\Omega_m$	$\delta_{\text{th}}$	$r_{\text{vir}}$ (kpc)	$c$ (kpc)	$H_0$ ( $\text{km s}^{-1} \text{Mpc}^{-1}$ )
0.3	340	273.2	8.9	65

## 2 The models used

### 2.1 The CDM NFW model

The CDM model tested by Xue et al. (2008) with several Blue Horizontal-Branch (BHB) halo stars consists of three components. Two of them are for the disk

$$U_{\text{disk}} = -\frac{GM_{\text{disk}} [1 - \exp(-\frac{r}{b})]}{r}, \quad (1)$$

where  $b$  is the disk scale length, and the bulge

$$U_{\text{bulge}} = -\frac{GM_{\text{bulge}}}{r + c_0}, \quad (2)$$

where  $c_0$  is the bulge scale radius. The third component is for the CDM NFW halo (Navarro et al. 1996)

$$U_{\text{NFW}} = -\frac{4\pi G \rho_s r_{\text{vir}}^3}{c^3 r} \ln \left( 1 + \frac{cr}{r_{\text{vir}}} \right), \quad (3)$$

with  $r_{\text{vir}}$  is the radius parameter and

$$\rho_s = \frac{\rho_{\text{cr}} \Omega_m \delta_{\text{th}}}{3} \frac{c^3}{\ln(1+c) - \frac{c}{1+c}}, \quad (4)$$

in which  $\Omega_m$  is the fraction of matter (including baryons and DM) to the critical density,  $\delta_{\text{th}}$  is critical overdensity of the virialized system,  $c$  is the concentration parameter, and

$$\rho_{\text{cr}} = \frac{3H_0^2}{8\pi G} \quad (5)$$

is the critical density of the Universe determined by the Hubble parameter  $H_0$  at redshift 0. The values used for the parameters entering Eq. (1) and Eq. (2) are in Table 1; those entering Eq. (3) are in Table 2.

### 2.2 The logarithmic CDM halo

Another model widely used consists of the Miyamoto & Nagai (1975) disk

$$U_{\text{disk}} = -\frac{\xi GM_{\text{disk}}}{\sqrt{x^2 + y^2 + (k + \sqrt{z^2 + B^2})^2}}, \quad (6)$$

**Table 3** Parameters of the logarithmic CDM halo model; values by Law et al. (2005).

$\xi$	$k$ (kpc)	$B$ (kpc)	$C$ (kpc)	$v_{\text{halo}}$ ( $\text{km s}^{-1}$ )	$d$ (kpc)
1	6.5	0.26	0.7	114	12

where  $k$  and  $B$  are the disk scale length and the disk scale height, respectively, the Plummer (1911) bulge

$$U_{\text{bulge}} = -\frac{GM_{\text{bulge}}}{r + C}, \quad (7)$$

where  $C$  is the bulge scale radius, and the logarithmic CDM halo (Binney & Tremaine 1987)

$$U_{\text{halo}} = v_{\text{halo}}^2 \ln(r^2 + d^2), \quad (\text{spherical halo}) \quad (8)$$

where  $d$  is the DM halo scale length and  $v_{\text{halo}}$  describes the DM halo dispersion speed (which is related to the total DM halo mass). The parameters's values are in Table 3.

The masses of the disk and the bulge used by Law et al. (2005) are those by Johnston et al. (1999):  $M_{\text{disk}} = 1 \times 10^{11} M_{\odot}$ ,  $M_{\text{bulge}} = 3.4 \times 10^{10} M_{\odot}$  yielding a total baryonic mass of  $M = 1.34 \times 10^{11} M_{\odot}$ ; however, such a value is almost twice the most recent estimate ( $M = 6.5 \times 10^{10} M_{\odot}$ ) by McGaugh (2008) who includes the gas mass as well and yield  $M_{\text{disk}} = 2.89 \times 10^{10} M_{\odot}$  and  $M_{\text{bulge}} = 2.07 \times 10^{10} M_{\odot}$ . The model of Eqs. (6)–(8), with the parameter values by Law et al. (2005) and Johnston et al. (1999), has been recently used by Willett et al. (2009) to study the motion of the Grillmair & Dionatos (2006) tidal stellar stream at galactocentric distance of  $r \approx 16$ –18 kpc; Read & Moore (2005) used it to study the motion of the tidal debris of the Sagittarius dwarf at 17.4 kpc from the center of MW. More specifically, the CDM halo model of Eq. (8) corresponds to a CDM halo mass of

$$M_{\text{halo}} = \frac{2v_{\text{halo}}^2 r^3}{G(r^2 + d^2)}, \quad (9)$$

so that

$$M_{\text{halo}}(r = 60 \text{ kpc}) = 3.5 \times 10^{11} M_{\odot}, \quad (10)$$

in agreement with the value by Xue et al. (2008)

$$M_{\text{halo}}(r = 60 \text{ kpc}) = (4.0 \pm 0.7) \times 10^{11} M_{\odot}. \quad (11)$$

### 2.3 Modified Newtonian Dynamics

MOND postulates that for systems experiencing total gravitational acceleration  $A < A_0$ , with (Begeman et al. 1991)

$$A_0 = (1.2 \pm 0.27) \times 10^{-10} \text{ m s}^{-2}, \quad (12)$$

$$A \rightarrow A_{\text{MOND}} = -\frac{\sqrt{A_0 GM}}{r}. \quad (13)$$

More precisely, it holds

$$A = \frac{A_{\text{Newton}}}{\mu(X)}, \quad X \equiv \frac{A}{A_0}; \quad (14)$$

$\mu(X) \rightarrow 1$  for  $X \gg 1$ , i.e. for large accelerations (with respect to  $A_0$ ), while  $\mu(X) \rightarrow X$  yielding Eq. (13) for  $X \ll 1$ , i.e. for small accelerations. Concerning the interpolating function  $\mu(X)$ , it recently turned out that the simple form (Famaey & Binney 2005)

$$\mu(X) = \frac{X}{1+X} \quad (15)$$

yields very good results in fitting the terminal velocity curve of MW, the rotation curve of the standard external galaxy NGC 3198 (Famaey & Binney 2005; Zhao & Famaey 2006; Famaey et al. 2007) and of a sample of 17 high surface brightness, early-type disc galaxies (Sanders & Noordermeer 2007); Eq. (14) becomes

$$A = \frac{A_{\text{Newton}}}{2} \left( 1 + \sqrt{1 + \frac{4A_0}{A_{\text{Newton}}}} \right) \quad (16)$$

with Eq. (15). Thus, in the following we will use Eq. (16).

## 2.4 MODIFIED GRAVITY

MOG is a fully covariant theory of gravity which is based on the existence of a massive vector field coupled universally to matter. The theory yields a Yukawa-like modification of gravity with three constants which, in the most general case, are running; they are present in the theory's action as scalar fields which represent the gravitational constant, the vector field coupling constant, and the vector field mass. An approximate solution of the MOG field equations by Moffat & Toth (2009) allows to compute their values as functions of the source's mass. The resulting Yukawa-type modification of the inverse-square Newton's law in the gravitational field of a central mass  $M$  is

$$A = -\frac{G_N M}{r^2} \{1 + \alpha [1 - (1 + \mu r) \exp(-\mu r)]\}, \quad (17)$$

with

$$\alpha \simeq \frac{M}{(\sqrt{M} + C'_1)^2} \left( \frac{G_\infty}{G_N} - 1 \right), \quad (18)$$

$$\mu \simeq \frac{C'_2}{\sqrt{M}}, \quad (19)$$

where  $G_N$  is the Newtonian gravitational constant and

$$G_\infty \simeq 20 G_N, \quad (20)$$

$$C'_1 \simeq 25\,000 \sqrt{M_\odot}, \quad (21)$$

$$C'_2 \simeq 6\,250 \sqrt{M_\odot} \text{ kpc}^{-1}. \quad (22)$$

Such values have been obtained by Moffat & Toth (2009) as a result of the fit of the velocity rotation curves of some galaxies in the framework of the searches for an explanation of the rotation curves of galaxies without resorting to CDM. The validity of Eq. (17) in the Solar System has been recently questioned by Iorio (2008).

For  $M = 6.5 \times 10^{10} M_\odot$  we have the values of Table 4.

**Table 4** MOG parameters  $\alpha$  and  $\lambda$  for  $M = 6.5 \times 10^{10} M_\odot$ .

$\alpha$	$\lambda$
–	(kpc)
16	41

**Table 5** Galactocentric initial conditions for the Sun (Reid et al. 2009); the positive  $y$  axis is directed from the Galactic Center (GC) to the Sun, the positive  $x$  axis is directed toward the Galactic rotation, the positive  $z$  axis is directed toward the North Galactic Pole (NGP). We have used  $\Theta_0 = 268 \text{ km s}^{-1}$  (Reid et al. 2009) for the rotation speed of LSR, and  $U_0 = 10.3 \text{ km s}^{-1}$ ,  $V_0 = 15.3 \text{ km s}^{-1}$ ,  $W_0 = 7.7 \text{ km s}^{-1}$  for the standard solar motions toward GC,  $\ell = 90^\circ$ , and NGP, respectively; thus, with our conventions,  $\dot{x}_0 = V_0 + \Theta_0$ ,  $\dot{y}_0 = -U_0$ ,  $\dot{z}_0 = W_0$ . See Fig. 7 of Reid et al. (2009).

$x_0$	$y_0$	$z_0$	$\dot{x}_0$	$\dot{y}_0$	$\dot{z}_0$
(kpc)	(kpc)	(kpc)	(km s <sup>-1</sup> )	(km s <sup>-1</sup> )	(km s <sup>-1</sup> )
0	8.5	0.02	15.3 + 268	-10.3	7.7

## 3 Solar motions backward in time

We will numerically integrate with MATHEMATICA<sup>1</sup> the Sun's equations of motion in Cartesian rectangular coordinates for  $-4.5 \text{ Gyr} \leq t \leq 0$  with the initial conditions of Table 5; in it we use the recently estimated value  $\Theta_0 = 268 \text{ km s}^{-1}$  for the rotation speed of the Local Standard of Rest (LSR) (Reid et al. 2009).

We will use both the NFW and logarithmic halo models for CDM which have been tested independently of the solar motion itself. In particular, we will numerically integrate the three scalar differential equations, written in Cartesian coordinates, corresponding to the vector differential equation

$$\frac{d^2 \mathbf{r}}{dt^2} = -\nabla U, \quad (23)$$

where  $U$  is the sum of Eqs. (1)–(3) with the values of Table 2 in the first case (NFW), and of Eqs. (6)–(8) with the values of Table 3 in the second case (logarithmic); we use the figures of Table 1 in both cases. For the two models of modified gravity considered we will put the Cartesian components of Eq. (16) (MOND) and Eq. (17) (MOG) in the right-hand-sides of the differential equations to be integrated. Concerning MOND, let us note that Eq. (14), from which Eq. (16) has been derived by means of Eq. (15) for  $\mu(X)$ , strictly holds for co-planar, spherically and axially symmetric mass distributions; otherwise, the full modified (non-relativistic) Poisson equation (Bekenstein & Milgrom 1984)

$$\nabla \cdot \left[ \mu \left( \frac{|\nabla U|}{A_0} \right) \nabla U \right] = 4\pi G \rho \quad (24)$$

must be used. However, in this case, the baryonic mass distributions of the bulge and the disk (see Eqs. 1–2 and Eqs.

<sup>1</sup> We will use the default options of NDSolve.

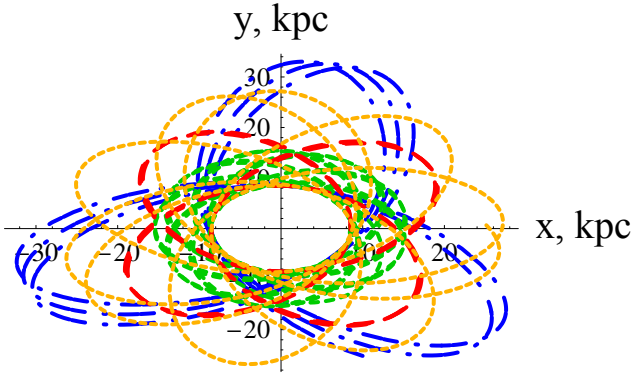


**Fig. 1** (online colour at: [www.an-journal.org](http://www.an-journal.org)) Section in the  $\{x, y\}$  plane of the numerically integrated trajectories of the Sun for a) CDM logarithmic halo (dash-dotted blue line), b) CDM NFW halo (dotted yellow line) c) MOND with  $\mu = X/(1 + X)$  (dashed green line), d) MOG (dashed red line). The time span is  $-4.5 \text{ Gyr} \leq t \leq 0$ . The initial conditions are those of Table 5 with  $\Theta_0 = 268 \text{ km s}^{-1}$  (Reid et al. 2009).

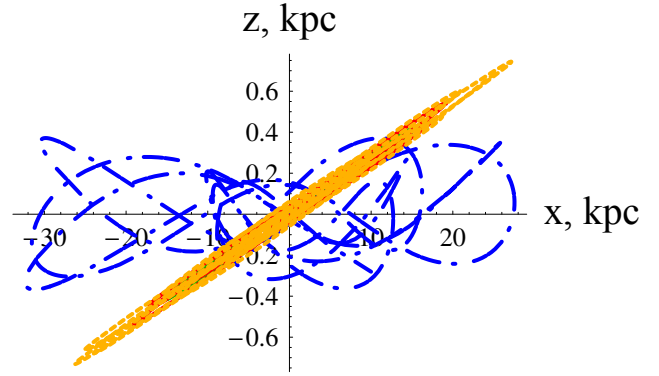


**Fig. 2** (online colour at: [www.an-journal.org](http://www.an-journal.org)) Section in the  $\{x, z\}$  plane of the numerically integrated trajectories of the Sun for a) CDM logarithmic halo (dash-dotted blue line), b) CDM NFW halo (dotted yellow line), c) MOND with  $\mu = X/(1 + X)$  (dashed green line), d) MOG (dashed red line). The time span is  $-4.5 \text{ Gyr} \leq t \leq 0$ . The initial conditions are those of Table 5 with  $\Theta_0 = 268 \text{ km s}^{-1}$  (Reid et al. 2009).

**Table 6** Galactocentric coordinates and distance of the Sun at  $t = -4.5 \text{ Gyr}$  according to our numerical integrations of the equations of motion in CDM (logarithmic halo), CDM (NFW halo), MOND and MOG for  $\Theta_0 = 268 \text{ km s}^{-1}$  (Reid et al. 2009). The initial conditions of Table 5 have been used.

Model	$x$ (kpc)	$y$ (kpc)	$z$ (kpc)	$r$ (kpc)
CDM log	9.9	-25.2	-0.3	27.1
CDM NFW	25.1	0.7	0.7	25.1
MOND ( $\mu = \frac{X}{1+X}$ )	4.4	11.1	0.1	12.0
MOG	15.4	-3	0.4	15.7

6–7) just satisfy the symmetry conditions that allow to use Eq. (14). Moreover,  $A_{\text{Newton}}/A_0 \approx 1$  for  $M = 6.5 \times 10^{10} M_\odot$ . This allows to neglect the so-called External Field Effect (EFE) (Sanders & McGaugh 2002; Milgrom 2008) because it should amount to about  $A_e/A_0 = 0.01\text{--}0.02$  for MW (Wu et al. 2008). Indeed, it can be shown that, for Eq. (15), the MOND acceleration, including EFE, is

$$A = \frac{A_{\text{Newton}}}{2} \left[ 1 - \frac{A_e}{A_{\text{Newton}}} + \sqrt{\left( 1 - \frac{A_e}{A_{\text{Newton}}} \right)^2 + \frac{4A_0}{A_{\text{Newton}}} \left( 1 + \frac{A_e}{A_0} \right)} \right], \quad (25)$$

which just reduces to Eq. (16) when  $A_e \ll A_{\text{Newton}}$ ,  $A_e \ll A_0$ , as in this case.

In Figs. 1–3 we plot the orbital sections in the Galactocentric coordinate planes of the numerically integrated trajectories of the Sun from now to 4.5 Gyr ago.

The orbital trajectories of the Sun are quite different in CDM, MOND and MOG; the largest spatial extension occur for the CDM models, especially for the one characterized by the CDM logarithmic halo. The Galactocentric coordinates and distances of the Sun at  $t = -4.5 \text{ Gyr}$  are quoted

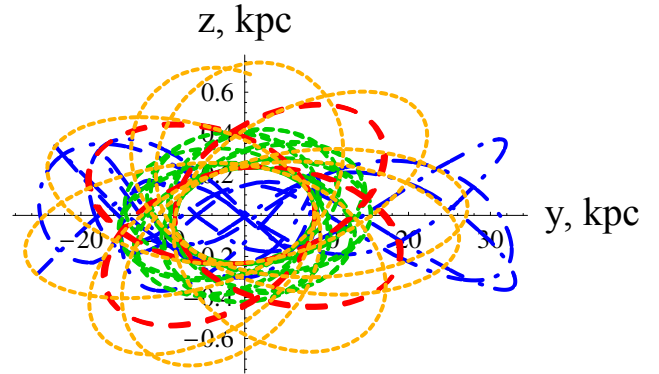


**Fig. 3** (online colour at: [www.an-journal.org](http://www.an-journal.org)) Section in the  $\{y, z\}$  plane of the numerically integrated trajectories of the Sun for a) CDM logarithmic halo (dash-dotted blue line), b) CDM NFW halo (dotted yellow line), c) MOND with  $\mu = X/(1 + X)$  (dashed green line), d) MOG (dashed red line). The time span is  $-4.5 \text{ Gyr} \leq t \leq 0$ . The initial conditions are those of Table 5 with  $\Theta_0 = 268 \text{ km s}^{-1}$  (Reid et al. 2009).

in Table 6. It can be noted that the models considered place the birth of the Sun from a minimum of 12.0 kpc (MOND) to a maximum of 25–27 kpc (CDM) from GC. This may pose problems concerning the birth of the Earth itself and the development of complex life on it because of, e.g., the presumable low level of metallicity (the amount of elements heavier than hydrogen and helium) in so distant regions. For a discussion and the implications of the concept of Galactic Habitable Zone (GHZ), see Lineweaver et al. (2004), Gonzalez (2005), and Prantzos (2008). In particular, see Fig. 5 by Prantzos (2008) which shows that the probability of having Earth formed 4 and 8 Gyr after the formation of MW, which roughly corresponds to the birth of the Sun by assuming a Milky Way age of about 10–12 Gyr, is practically null at Galactocentric distances larger than 10–15 kpc.



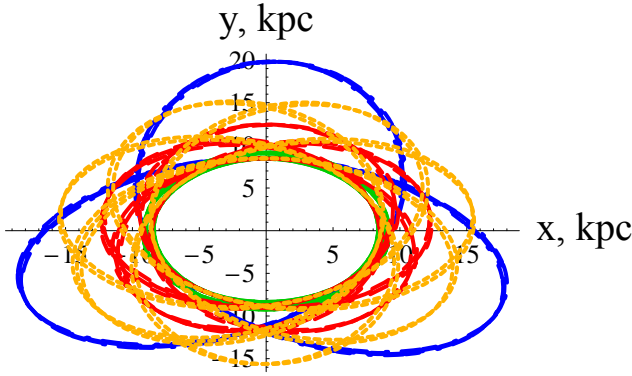


**Fig. 4** (online colour at: [www.an-journal.org](http://www.an-journal.org)) Section in the  $\{x, y\}$  plane of the numerically integrated trajectories of the Sun for a) CDM logarithmic halo (dash-dotted blue line), b) CDM NFW halo (dotted yellow line), c) MOND with  $\mu = X/(1 + X)$  (dashed green line), d) MOG (dashed red line). The time span is  $-4.5 \text{ Gyr} \leq t \leq 0$ . The initial conditions are those of Table 5 with the IAU recommended value  $\Theta_0 = 220 \text{ km s}^{-1}$ .

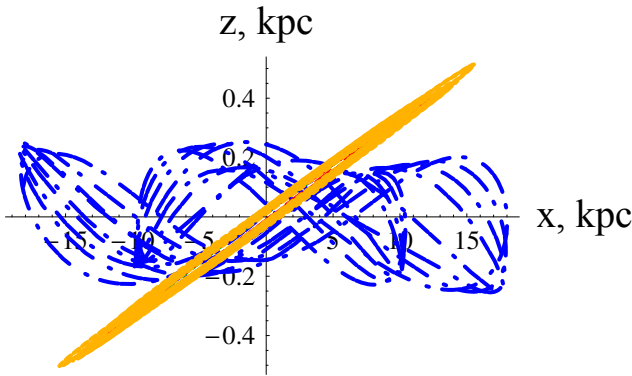


**Fig. 5** (online colour at: [www.an-journal.org](http://www.an-journal.org)) Section in the  $\{x, z\}$  plane of the numerically integrated trajectories of the Sun for a) CDM logarithmic halo (dash-dotted blue line), b) CDM NFW halo (dotted yellow line), c) MOND with  $\mu = X/(1 + X)$  (dashed green line), d) MOG (dashed red line). The time span is  $-4.5 \text{ Gyr} \leq t \leq 0$ . The initial conditions are those of Table 5 with the IAU recommended value  $\Theta_0 = 220 \text{ km s}^{-1}$ .

In Figs. 4–6 we repeat the same integrations by using the IAU recommended value  $\Theta_0 = 220 \text{ km s}^{-1}$ . The Galactocentric coordinates and distances of the Sun at  $t = -4.5 \text{ Gyr}$  for  $\Theta_0 = 220 \text{ km s}^{-1}$  are quoted in Table 7. Now the situation is quite different because, apart from the logarithmic CDM halo, all the other models locate the birth of the Sun at 8.8–9.3 kpc from GC.

#### 4 Summary and conclusions

By using the latest kinematical determinations of the full 3D solar motion in the Milky Way, implying a LSR rotation of  $\Theta_0 = 268 \text{ km s}^{-1}$ , we used them as initial conditions for numerically integrating the equations of motion of the Sun backward in time ( $-4.5 \text{ Gyr} \leq t \leq 0$ ) in Newtonian me-

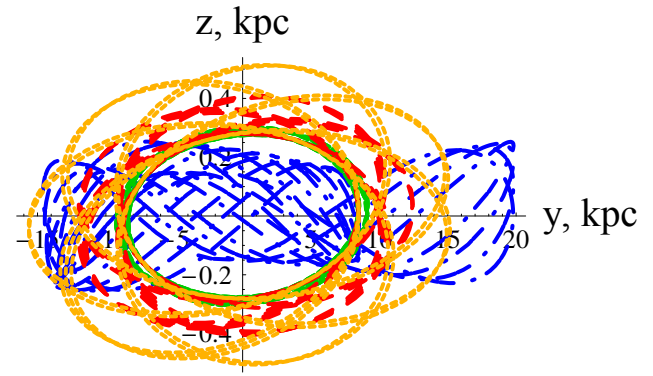


**Fig. 6** (online colour at: [www.an-journal.org](http://www.an-journal.org)) Section in the  $\{y, z\}$  plane of the numerically integrated trajectories of the Sun for a) CDM logarithmic halo (dash-dotted blue line), b) CDM NFW halo (dotted yellow line), c) MOND with  $\mu = X/(1 + X)$  (dashed green line), d) MOG (dashed red line). The time span is  $-4.5 \text{ Gyr} \leq t \leq 0$ . The initial conditions are those of Table 5 with the IAU recommended value  $\Theta_0 = 220 \text{ km s}^{-1}$ .

**Table 7** Galactocentric coordinates and distance of the Sun at  $t = -4.5 \text{ Gyr}$  according to our numerical integrations of the equations of motion in CDM (logarithmic halo), CDM (NFW halo), MOND, and MOG. The initial conditions of Table 5 have been used with the IAU recommended value  $\Theta_0 = 220 \text{ km s}^{-1}$ .

Model	$x$ (kpc)	$y$ (kpc)	$z$ (kpc)	$r$ (kpc)
CDM log	−18.1	−4.7	0.1	18.8
CDM NFW	7.1	−5.2	0.2	8.8
MOND ( $\mu = \frac{x}{1+x}$ )	6.1	6.5	0.2	8.9
MOG	9.2	1.1	0.3	9.3

chanics with two models for the CDM halo, in MOND and in MOG. As a result, the orbital trajectories are not circular and differ each other, with the CDM models yielding the widest spatial extensions of the Sun's orbit. It turns out that for  $t = -4.5 \text{ Gyr}$  the Sun is at quite large Galactocentric distances ( $r \approx 12\text{--}27 \text{ kpc}$  depending on the models). Instead, by using the standard IAU value  $\Theta_0 = 220 \text{ km s}^{-1}$  the situation is different: the orbits are less wide and at  $t = -4.5 \text{ Gyr}$  the Sun is at 8.8–9.3 kpc from GC for almost all the models considered.

*Acknowledgements.* I thank M. Masi for useful references and discussions.

#### References

- Begeman, K., Broeils, A., Sanders, R.: 1991, MNRAS 249, 523
- Bekenstein, J., Milgrom, M.: 1984, ApJ 286, 7
- Binney, J., Tremaine, S.: 1987, *Galactic Dynamics*, Princeton Univ. Press, Princeton, NY, p. 747
- Bosma, A.: 1981, AJ 86, 1791
- Famaey, B., Binney, J.: 2005, MNRAS 363, 603
- Famaey, B., Gentile, G., Bruneton, J.-P., Zhao, H.: 2007, Phys Rev D 75, 063002

- Gonzalez, G.: 2005, OLEB 35, 555
- Grillmair, C., Dionatos, O.: 2006, ApJ 643, L17
- Iorio, L.: 2008, Schol. Res. Exchange 2008, 238385
- Johnston, K., Majewski, S., Siegel, M., Reid, I., Kunkel, W.: 1999, AJ 118, 1719
- Law, D., Johnston, K., Majewski, S.: 2005, ApJ 619, 807
- Lineweaver, C., Fenner, Y., Gibson, B.: 2004, Sci 303, 59
- McGaugh, S.: 2008, ApJ 683, 137
- Milgrom, M.: 1983a, ApJ 270, 365
- Milgrom, M.: 1983b, ApJ 270, 371
- Milgrom, M.: 1983c, ApJ 270, 384
- Milgrom, M.: 2008, Talk presented at the XIX Rencontres de Blois, <http://arxiv.org/abs/0801.3133v2>
- Miyamoto, M., Nagai, R.: 1975, PASJ 27, 533 (MN)
- Moffat, J., Toth, V.: 2008, ApJ 680, 1158
- Moffat, J., Toth, V.: 2009, CQG 26, 085002
- Navarro, J.F., Frenk, C.S., White, S.D.M.: 1996, ApJ, 462, 563
- Persic, M., Salucci, P., Stel, F.: 1996a, MNRAS 281, 27
- Persic, M., Salucci, P., Stel, F.: 1996b, MNRAS 283, 1102
- Plummer, H.C.: 1911, MNRAS 71, 460
- Prantzos, N.: 2008, SSRv 135, 313
- Read, J., Moore, B.: 2005, MNRAS 361, 971
- Reid, M.J., Menten, K.M., Zheng, X.W., Brunthaler, A., et al.: 2009, ApJ 700, 137
- Rubin, V.: 1983, Sci 220, 1339
- Rubin, V., Ford, W., Thonnard, N., Burstein, D.: 1982, ApJ 261, 439
- Sanders, R., McGaugh, S.: 2002, ARA&A 40, 263
- Sanders, R., Noordermeer, E.: 2007, MNRAS 379, 702
- Willett, B., Newberg, H., Zhang, H., Yanny, B., Beers, T.: 2009, ApJ 697, 207
- Wu, X., Famaey, B., Gentile, G., Perets, H., Zhao, H.: 2008, MNRAS 386, 2199
- Xue, X.-X., Rix, H.-W., Zhao, G., Re Fiorentin, P., et al.: 2008, ApJ 684, 1143
- Zhao, H., Famaey, B.: 2006, ApJ 638, L9
- Zwicky, F.: 1933, AcHPh 6, 110